SUPPLEMENTAL METHODS

Invasive Hemodynamics

Under fluoroscopic guidance, an LV pressure-conductance catheter (5F, 12 electrodes, 7mm spacing, MPVS Ultra, Millar Instruments, Houston, Texas, USA) was positioned in the apex. To calibrate the catheter, the blood conductivity (ρ) and the parallel conductance (V_c) (15% hypertonic saline infusion) were performed prior to each study. Steady-state data was acquired under spontaneous heart rate (HR) for approximately 15 beats prior to inferior vena cava (IVC) occlusion. A maximum of three IVC occlusions was performed to collect stable data (≤ 20 beats). Ventilator tidal volume was set to zero during this time to eliminate respiratory artifact. This procedure was replicated under the administration of 2.5ug/kg/min DOB infusion at baseline, 3Mo post MI ± RBX. Hemodynamic analysis was performed offline using LabChart software (ADInstruments, Colorado Springs, Colorado, USA).

End diastole (ed) was defined using an end-diastolic pressure (EDP) algorithm that considers the maximum pressure, the preceding minimum pressure and the maximal change in pressure/change in time (dP/dT max.). End systole (es) was defined as the point of maximum pressure-volume ratio. The end-diastolic pressure-volume relationship (EDPVR) was derived from a curve fit (exponential) of the raw data collected during an inferior vena cava (IVC) occlusion, where $P_{ed} = \alpha \times e^{\beta x LVVed}$. The end-systolic pressure-volume relationship (ESPVR) is derived from the calculated end-systolic elastance (E_{es}) "slope" of the ES points acquired during IVC occlusion and the calculated volume axis intercept (V_0). It is imperative to compare changes in both the E_{es} and V_0, as E_{es} is a load dependent measurement of contractility (1). To determine changes in capacitance or changes in LV size we calculated the LV volumes at an end-diastolic pressure of 10mmHg (LV $VP_{ed}10$). We performed the same measurement at an end

systolic pressure of 100mmHg (LV $VP_{es}100$). The isovolumic relaxation constant τ (ms) was calculated as described by Weiss (2). Upon analysis, changes in slope (E_{es}) and volume intercept (V_0) were considered in regards to the ESPVR and EDPVR. We used the analytical methodology described previously (1) to generate a set of variables that can be used, so long as either of the raw data (Ees and/or V_0) are significantly different from one another. Then the mean data was plotted for a given set of pressures. Hemodynamics data were analyzed using the mixed-effects regression model with dummy variables (a user determined set of pressures (eg. 60, 70, 80…120) is the standard to take into consideration the interdependence of the E_{es} and V_0 (1). If the statistical test indicated differences between groups, then the average slope ± SEM and intercept was plotted on a common set of axes.

Tissue Processing & Gross Morphometric Analysis

Cardiectomy was performed under general anesthesia and gross morphometry was performed as previously described (3). Briefly, the heart was weighed and the basal two-thirds fixed via perfusion with 2-liters of 10% formalin. The bottom third was taken for molecular analysis. The fixed portion was sectioned into short-axis slices. Each slice was measured for mean thickness prior to further processing. The basal surface of each slice was photographed using a Nikon DS-F11 camera. Sections from infarct zone, border zone and remote zone were processed for histological analysis and stained for Masson's trichrome (Sigma-Aldrich Cat#: HT15). Wheat germ agglutinin ([WGA] Life Technologies Cat#: W11262) staining was performed to observed myocyte cross-sectional area (CSA).

The scar area was identified by the extracellular matrix deposition, while the viable area was healthy tissue; both were measured using NIH Image J software. The scar volume was calculated by multiplying the scar area of each slice by the average thickness, this calculation

was also performed for the viable area. The percent scar volume of each heart was determined by adding the volumes of all slices and dividing by the total scar volume. Tissue samples were also collected for molecular analysis. Transmural slices from the mid-myocardial anterior (infarct), lateral (border) and posterior (remote) walls of the left ventricle were flash frozen in liquid nitrogen and stored at -80^{o}C for further analysis.

Protein Isolation and Fractionation for Western Blot Analysis

Tissue was placed in 1ml of pre-chilled 'cytoplasmic extraction buffer' and homogenized for 10-20 strokes. Homogenate was incubated on ice for 10 minutes, then transferred to a 1.5ml Eppendorf tube and centrifuged at 4^{o}C for five minutes at 500xg. We then immediately transferred supernatant into another 1.5ml Eppendorf tube (cytoplasmic fraction). The pellet was then resuspended in 650µl of 'membrane extraction buffer' and incubated at 4^{o}C for ten minutes with continuous gentle mixing. Next, the samples were centrifuged at 4^{o}C for 5minutes at 3000xg. The supernatant was collected and placed in another 1.5ml Eppendorf tube. The pellet was then discarded and the cytoplasmic and membrane fractions were stored for western blot analysis.

Western blots were performed using the LICOR Systems general protocol. Samples were run on a 12% SDS-page gel and transferred overnight to 0.45µm nitrocellulose. Blocking was performed and primary antibody for was incubated for 1hr at room temperature. The blots were then washed three times and incubate in LICOR IRDye® 800CW anti-rabbit secondary (LICOR, Cat#: 926-32213) for 30 minutes. Membranes were washed then imaged using the LICOR System and analyzed. Quantification of band intensity was performed using LICOR Image Studio software. PKCα activation involves its translocation from the cytoplasm to the membrane (4). Total PKCα activation was presented as a percentage of membrane/cytoplasmic fraction.

Activation was determined by measuring the ratio of membrane bound PKCα to cytosolic abundance. Primary antibodies were as follows: PKCα (Sigma-Aldrich Cat#: P4334), PKCα pT638 (GeneTex, Cat#: GTX61075), GAPDH (AbD Serotec Cat#: MCA4739), PLN (Millipore, Cat#: 05-205), PLN pSer16 & pThr17 (Badrilla, Cat#: A010-12 & A010-13 respectively).

Statistics

All data analyses were performed using SAS version 9.3 (SAS Institute, NC, USA). Data were presented as mean ± SEM and analyzed mainly within each treatment group over time (MI or CON= Control), except for when the comparisons between the treatment groups were made for variables such as heart to body weight ratio. Heart to body weight ratio and cross-sectional area were analyzed using a two-sample t-test to show the balance between the two treatment groups. Changes post MI in echocardiographic and electrocardiogram parameters measured at baseline, 1Mo, 2Mo, and 3Mo post MI were analyzed using the mixed-effects model approach for the repeated measurements over time and the comparisons within the treatment group between each of the three post MI time points and the baseline were made simultaneously via the Dunnett-Hsu or Bonferroni adjustment for the p-value for other sets of pairwise comparisons of interest when appropriate. This modeling approach took into account the within-animal correlation among repeated measurements over time via a flexible structure for variance components, affording different magnitude of variability across the different time points within the treatment group. Within-group changes in endpoints of interest between 3Mo post MI ± RBX as reported in this supplement were analyzed using the non-parametric sign rank test due to the relative small sample sizes. Hemodynamics data were analyzed using the mixed-effects regression model in a similar fashion as described previously (5). Western blot analysis was performed using Mann–

Whitney–Wilcoxon test. For all analyses, a two-sided p-value of < 0.05 was considered statistically significant.

REFERENCES

1. Burkhoff D, Mirsky I, Suga H. Assessment of systolic and diastolic ventricular properties via pressure-volume analysis: a guide for clinical, translational, and basic researchers. Am J Physiol Heart Circ Physiol2005 Aug;289(2):H501-12.

2. Weiss JL, Frederiksen JW, Weisfeldt ML. Hemodynamic determinants of the time-course of fall in canine left ventricular pressure. J Clin Invest1976 Sep;58(3):751-60.

3. Duran JM, Taghavi S, Berretta RM, Makarewich CA, Sharp Iii T, Starosta T, Udeshi F, George JC, Kubo H, Houser SR. A Characterization and Targeting of the Infarct Border Zone in a Swine Model of Myocardial Infarction. Clinical and Translational Science2012;5(5):416-21.

4. Bowling N, Walsh RA, Song G, Estridge T, Sandusky GE, Fouts RL, Mintze K, Pickard T, Roden R, Bristow MR, Sabbah HN, Mizrahi JL, Gromo G, King GL, Vlahos CJ. Increased Protein Kinase C Activity and Expression of Ca2+-Sensitive Isoforms in the Failing Human Heart. Circulation1999 January 26, 1999;99(3):384-91.

5. Schwarzl M, Hamdani N, Seiler S, Alogna A, Manninger M, Reilly S, Zirngast B, Kirsch A, Steendijk P, Verderber J, Zweiker D, Eller P, Hofler G, Schauer S, Eller K, Maechler H, Pieske BM, Linke WA, Casadei B, Post H. A porcine model of hypertensive cardiomyopathy: implications for heart failure with preserved ejection fraction. Am J Physiol Heart Circ Physiol2015 Nov;309(9):H1407-18.

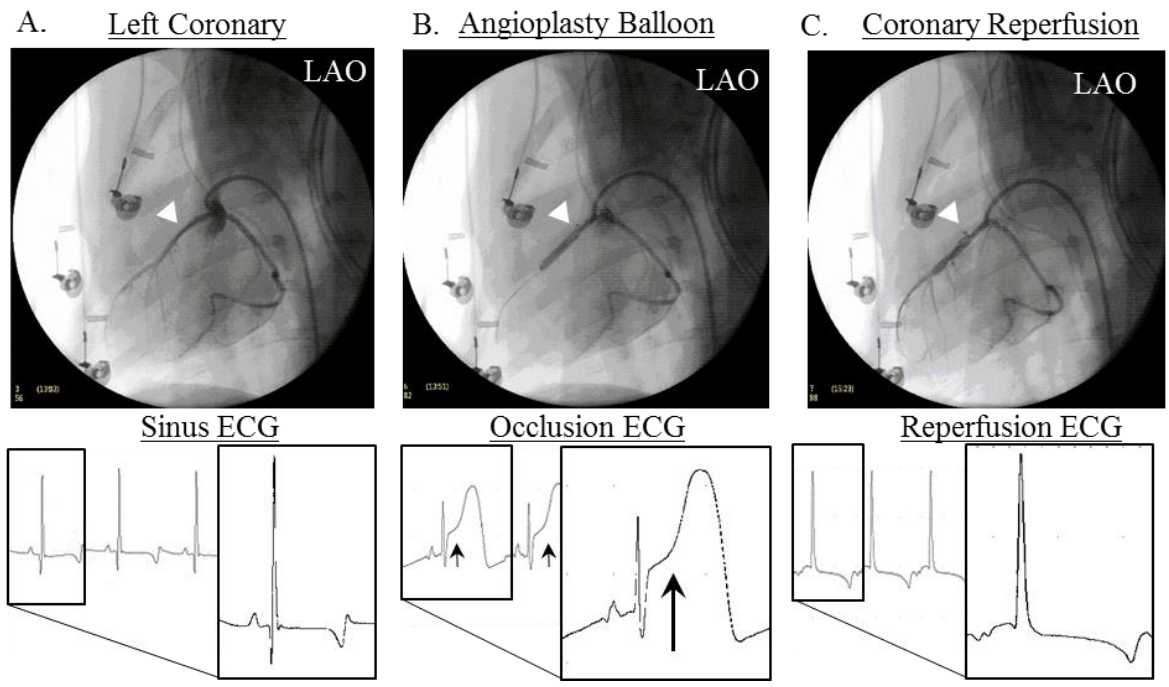

Supplemental Figure 1. Coronary Angiography and Electrocardiogram during MI procedure. Angiography was performed in the left anterior oblique (LAO) position. White arrow head indicates the LAD coronary artery and angioplasty balloon placement. **(A)** Pre-MI coronary angiogram displays the LAD and the circumflex distribution of the left coronary artery, also showing a sinus rhythm in the electrocardiogram (ECG). **(B)** Angiogram demonstrating angioplasty balloon occlusion of the LAD distribution with cessation of flow just distal the white arrow head. ST-segment elevation observed in the ECG, consistent with an LAD occlusion and MI of the anterior/apical LV wall. **(C)** Coronary angiogram demonstrating reperfusion of the occluded vessel after removal of the angioplasty balloon with resolution to the ST-segment elevation in the ECG.

Table 1.0 Invasive Hemodynamics

	Baseline (n = 5)		3MO Post MI (n = 5)		
	(-) DOB	(+) DOB	(-) DOB	(+) DOB	(+) RBX
Heart Rate (bpm)					
Mean	87.85	90.55	96.89	91.05	120.21
±SEM	10.75	10.77	15.83	9.88	30.89
$Volume_{es}$ (mL)					
Mean	10.67	8.27	51.6*	39.06*†	24.5*†
±SEM	2.67	2.55	3.98	8.56	3.26
$Volume_{ed}$ (mL)					
Mean	30.31	27.65	70.56*	62.48*	42.74†
±SEM	4.36	3.67	4.64	9.80	3.46
Stroke Volume (mL)					
Mean	21.06	21.96	26.25	28.55	22.86
±SEM	2.28	2.08	3.29	3.41	5.47
Ejection Fraction (%)					
Mean	71.61	79.39	35.55*	48.8†	50.61†
±SEM	4.16	5.21	2.52	6.92	8.13
dP/dt max (mmHg/s)					
Mean	1623.00	3435.00*	1238.56	2889.4*†	2063.25
±SEM	90.17	328.78	105.58	755.61	665.53
dP/dt min (mmHg/s)					
Mean	-1888.60	-1903.00	-1519.00	-1767.20	-1572.10
±SEM	200.20	213.72	83.94	156.45	344.86
End-systolic Elastance (E*es*)					
Mean	4.72	7.22*	3.14	4.06	4.86†
±SEM	0.40	0.39	0.61	0.72	0.42
Volume axis intercept (V_0)					
Mean	-4.89	-4.37	23.66*	18.64*	3.99†‡
±SEM	3.33	2.11	6.06	5.14	6.83
Pre-load Recruitable Stroke Work (PRSW)					
Slope					
Mean	62.46	87.75*	56.83	95.91*†	64.69
±SEM	5.44	5.42	10.54	16	10.63
Volume axis intercept (V_0)					
Mean	9.2	6.85	45.15*	43.67*	17.14†‡
±SEM	3.06	3.36	6.99	5.76	6.53

End-systole ($_{es}$), end-diastole ($_{ed}$), Stroke Volume (SV), Eleastance arterial (Ea), Maximal change in pressure over time (dP/dT max.), Minimal change in pressure over time (dP/dT min.), Volume at dP/dT max./min. (V@dP/dT max./min.), and relaxation constant (Tau). P-values were calculated using the sign rank test with a Bonferroni multiple comparisons corrections for the MI group for comparisons between baseline, three months post-MI and three months post-MI + RBX. $p \leq 0.05$ are significant. Indicates significant vs. Baseline (*); vs. 3MO Post MI (†); vs. 3MO Post MI + Dob. (‡)

Supplemental Table 2.0 Electrocardiogram Measurements

	Baseline (n=12)	*1Mo†* (n=12)	*2Mo†* (n=12)	*3Mo†* (n=12)	*3Mo + RBX ** (n=12)	*CON* (n=3)	*CON + RBX ** (n=3)
		Post MI					
Heart Rate (bpm)							
Mean ± SEM	110 ± 6.1	114 ± 5.4	107 ± 7.8	101 ± 6.1	131 ± 6.8[a]	104 ± 13.2	109 ± 1.5
PR Interval (ms)							
Mean ± SEM	104 ± 4.1	112 ± 3.3	115 ± 4.2	114 ± 3.1	105 ± 3.3[a]	119 ± 7.5	106 ± 5.8
QRS (ms)							
mean ± SEM	55 ± 0.7	56 ± 1.6	60 ± 1.2[a]	61 ± 1.2[b]	62 ± 0.9	57 ± 2.4	54.7 ± 2.5
QTc (ms)							
Mean ± SEM	391 ± 11.6	414 ± 8.3	437 ± 16.0	432 ± 10.0	441 ± 11.0	431 ± 10.6	428 ± 7.0

†- *P-values* were calculated using the sign rank test with a Bonferroni multiple comparisons corrections for the MI group for comparisons between baseline and each of the three post-MI time points (1, 2, and 3 months post MI).

* - Indicates that no multiple comparison corrections were made to the p-values for comparisons between 12 wks post-MI + RBX and 12 wks post-MI or Con (control animals) and CON + RBX.

P-values $= {}^{a}p < 0.05; {}^{b}p < 0.01$